JCI insight

Immunotoxin-mediated depletion of Gag-specific CD8+ T cells undermines natural control of Simian immunodeficiency virus

Jennifer Simpson, … , David A. Price, Jason M. Brenchley

JCI Insight. 2024. https://doi.org/10.1172/jci.insight.174168.

Research In-Press Preview AIDS/HIV

Antibody-mediated depletion studies have demonstrated that CD8+ T cells are required for effective immune control of SIV. However, this approach is confounded by several factors, including reactive CD4+ T cell proliferation, and further provides no specificity information. We circumvented these limitations by selectively depleting CD8+ T cells specific for the Gag epitope CTPYDINQM (CM9) via the administration of immunotoxin-conjugated tetrameric complexes of CM9/Mamu-A*01. Immunotoxin administration effectively depleted circulating but not tissuelocalized CM9-specific CD8+ T cells, akin to the bulk depletion pattern observed with antibodies directed against CD8. However, we found no evidence to indicate that circulating CM9-specific CD8+ T cells suppressed viral replication in Mamu-A*01+ rhesus macaques during acute or chronic progressive infection with a pathogenic strain of SIV. This observation extended to macaques with established infection during and after continuous antiretroviral therapy. In contrast, natural controller macaques experienced dramatic increases in plasma viremia after immunotoxin administration, highlighting the importance of CD8+ T cell-mediated immunity against CM9. Collectively, these data showed that CM9-specific CD8+ T cells were necessary but not sufficient for robust immune control of SIV in a nonhuman primate model and, more generally, validated an approach that could inform the design of next-generation vaccines against HIV-1.

Immunotoxin-mediated depletion of Gag-specific CD8$^+$ T cells undermines natural control of SIV

Jennifer Simpson[1], Carly E. Starke,[1,2] Alexandra M. Ortiz[1], Amy Ransier[3], Sam Darko[3], Sian Llewellyn-Lacey[4], Christine M. Fennessey[5], Brandon F. Keele[5], Daniel C. Douek[3], David A. Price[4,6], Jason M. Brenchley[1]

1. Barrier Immunity Section, Laboratory of Viral Diseases, National Institute of Allergy and Infectious Diseases, National Institutes of Health, Bethesda, MD 20892, USA.
2. Stem Cell and Gene Therapy Program, Fred Hutchinson Cancer Research Center, Seattle, WA 98109, USA.
3. Human Immunology Section, Vaccine Research Center, National Institute of Allergy and Infectious Diseases, National Institutes of Health, Bethesda, MD 20892, USA.
4. Division of Infection and Immunity, Cardiff University School of Medicine, University Hospital of Wales, Cardiff CF14 4XN, UK.
5. AIDS and Cancer Virus Program, Frederick National Laboratory for Cancer Research, National Cancer Institute, National Institutes of Health, Frederick, MD 21702, USA.
6. Systems Immunity Research Institute, Cardiff University School of Medicine, University Hospital of Wales, Cardiff CF14 4XN, UK.

Address correspondence to: Jason M. Brenchley, Barrier Immunity Section, Laboratory of Viral Diseases, Building 4, Room 201, 4 Memorial Drive, National Institute of Allergy and Infectious Diseases, National Institutes of Health, Bethesda, MD 20892, USA. Phone: +1 3014961498. Email: jbrenchl@niaid.nih.gov.

CONFLICT OF INTEREST STATEMENT

The authors have no conflicts of interest to declare.

ABSTRACT

Antibody-mediated depletion studies have demonstrated that $CD8^+$ T cells are required for effective immune control of SIV. However, this approach is potentially confounded by several factors, including reactive $CD4^+$ T cell proliferation, and further provides no information on epitope specificity, a likely determinant of $CD8^+$ T cell efficacy. We circumvented these limitations by selectively depleting $CD8^+$ T cells specific for the Gag epitope CTPYDINQM (CM9) via the administration of immunotoxin-conjugated tetrameric complexes of CM9/Mamu-A*01. Immunotoxin administration effectively depleted circulating but not tissue-localized CM9-specific $CD8^+$ T cells, akin to the bulk depletion pattern observed with antibodies directed against CD8. However, we found no evidence to indicate that circulating CM9-specific $CD8^+$ T cells suppressed viral replication in Mamu-A*01^+ rhesus macaques during acute or chronic progressive infection with a pathogenic strain of SIV. This observation extended to macaques with established infection during and after continuous antiretroviral therapy. In contrast, natural controller macaques experienced dramatic increases in plasma viremia after immunotoxin administration, highlighting the importance of $CD8^+$ T cell-mediated immunity against CM9. Collectively, these data showed that CM9-specific $CD8^+$ T cells were necessary but not sufficient for robust immune control of SIV in a nonhuman primate model and, more generally, validated an approach that could inform the design of next-generation vaccines against HIV-1.

INTRODUCTION

$CD8^+$ T cells are thought to be critical for immune control of HIV-1 and, in nonhuman primates, SIV (1–3). Infected cells display an array of viral peptide epitopes presented in the context of surface-expressed major histocompatibility complex (MHC) class I molecules that act as antigenic targets for recognition via uniquely encoded T cell receptors (TCRs) (4). In response to signals received during this process of molecular recognition, antigen-specific $CD8^+$ T cells undergo clonal expansion (5) and acquire effector functions, including cytotoxicity (6) and the ability to release proinflammatory cytokines, such as interferon (IFN)-γ and tumor necrosis factor (TNF) (6–9). The emergence of antigen-specific $CD8^+$ T cells with effector functionality has been associated temporally with the initial decline in viremia that occurs during acute infection with HIV-1 (10). Escape mutations in targeted epitopes also occur rapidly after infection (11–16), and disease progression is tightly linked with the expression of individual MHC class I molecules (17–20), which dictate the landscape of presentable antigens derived from HIV-1 and SIV. Effective immune control of viral replication is nonetheless rare, and most untreated individuals progress inexorably to AIDS (21).

Antibody-mediated depletion studies have provided direct evidence that $CD8^+$ T cells suppress viral replication during the acute and chronic phases of infection with SIV, the latter either in the absence or presence of continuous treatment with antiretroviral drugs (ARVs) (22–24). However, such bulk depletion of an entire lineage based on the expression of CD8, which can also include NK cells, introduces caveats to interpretation, feasibly extending to reactive $CD4^+$ T cell proliferation, which could potentially increase the number of target cells available for infection by SIV (25). To circumvent these issues, we selectively depleted $CD8^+$ T cells specific for the Gag

epitope CTPYDINQM (CM9), which is typically immunodominant in SIV-infected rhesus macaques expressing the appropriate restriction element, namely Mamu-A*01. This approach was enabled *in vivo* by conjugating saporin (26) with ultrapure recombinant tetrameric complexes of CM9/Mamu-A*01. Similar immunotoxin complexes have been used previously in mouse models (27) and, more recently, to deplete HIV-1-specific $CD8^+$ T cells *in vitro* (28).

Immunotoxin administration effectively depleted circulating CM9-specific $CD8^+$ T cells but less effectively depleted tissue-localized CM9-specific $CD8^+$ T cells, mirroring the pattern of wholesale depletion observed with antibodies directed against CD8. No measurable effects on viral replication were observed after immunotoxin administration during acute or chronic progressive infection, the latter irrespective of continuous treatment with ARVs. However, elevated plasma viral loads (VLs) were observed in natural controller macaques after immunotoxin administration, indicating that CM9-specific $CD8^+$ T cells can proactively suppress the replication of SIV.

RESULTS

CM9-specific CD8$^+$ T cells contribute to natural control of viremia during chronic infection with SIV

CD8$^+$ T cell responses directed against the immunodominant Mamu-A*01-restricted CM9 epitope (CTPYDINQM) are thought to play a key role in the containment of viral replication (29) as a consequence of biological and structural constraints that limit the options for mutational immune escape in this region of SIV Gag (30, 31). To test this notion, we administered a targeted immunotoxin to five Mamu-A*01$^+$ rhesus macaques with established SIVmac239 infection, aiming to deplete CM9-specific CD8$^+$ T cells, and measured the impact of this intervention among tissues and peripheral blood mononuclear cells (PBMCs) (**Figure 1A**). Two of these macaques had spontaneously controlled plasma VL to <10,000 copies/mL. After 4 days, CM9-specific CD8$^+$ T cell frequencies were substantially reduced among PBMCs (**Figure 1B**, **C**), but lesser effects were observed in tissues, including bronchoalveolar lavage (BAL) samples from the respiratory tract, jejunum, and lymph nodes (LNs) (**Figure 1D**). Depletion of CM9-specific CD8$^+$ T cells was associated with a 10-fold increase in plasma VL in one natural controller macaque (08D030) and a 2.5-fold increase in plasma VL in the other natural controller macaque (DGT4). No increases in plasma VL were observed in the three macaques with poor control of SIV (**Figure 1E**). After 17 days, set-point plasma VL was restored in macaques 08D030 and DGT4 (**Figure 1F**), paralleling the reconstitution of CM9-specific CD8$^+$ T cells among PBMCs (**Figure 1G**). Although formal statistical analysis was not possible, reflecting the rarity of spontaneous immune control in this model, these data suggested that CM9-specific CD8$^+$ T cells were largely redundant in macaques with unconstrained viral replication but nonetheless exerted potent antiviral activity in macaques with low set-point VLs.

Immunotoxin administration does not alter viral load kinetics during acute infection with SIV

To evaluate the impact of CM9-specific $CD8^+$ T cells on acute viral replication, we infected five Mamu-A*01^+ rhesus macaques with SIVmac239 (day 0) and administered the immunotoxin on days 7, 10, and 13. Immunotoxin was withheld from five control Mamu-A*01^+ rhesus macaques treated otherwise identically. The dosing and sampling schedules are depicted in **Figure 2A**. Immunotoxin administration transiently reduced the frequencies of CM9-specific and, to a lesser extent, total memory $CD8^+$ T cells among PBMCs (**Figure 2B**, **C** and **Supplemental Figure 1A**). In contrast, no significant depletion of CM9-specific $CD8^+$ T cells was observed in BAL, colon, jejunum, or LNs (**Supplemental Figure 1B**–**E**), and there was no evidence of reactive $CD4^+$ T cell proliferation among PBMCs (**Figure 2D**). Moreover, immunotoxin administration did not significantly affect plasma VL trajectories measured out to day 30 (**Figure 2E**) or $CD4^+$ T cell-associated VLs measured on days 10, 20, or 30 (**Figure 2F**). Despite the caveat of incomplete depletion, especially among tissues that typically sustain viral replication, these data suggested that CM9-specific $CD8^+$ T cells did not critically affect the natural course of acute infection with SIV.

Immunotoxin administration does not modulate the clonotypic repertoire of CM9-specific $CD8^+$ T cells during acute infection with SIV

The mobilization of distinct CM9-specific $CD8^+$ T cell clonotypes, defined by the expression of unique TCRs, has been associated with differential outcomes after acute infection with SIV (32). To determine if particular clonotypes were preferentially depleted by the immunotoxin, we isolated ultrapure populations of CM9-specific $CD8^+$ T cells directly *ex vivo* and sequenced the

corresponding rearranged TCRβ chain (*TRB*) genes using a high-throughput approach (33). Repertoires were compared across anatomical sites sampled from control macaques (n = 4–5) or immunotoxin-treated macaques (n = 4–5) at comparable time points during the acute study. Logo analysis of the third complementarity-determining region (CDR3β), which canonically plays a key role in antigen recognition, revealed similar amino acid chemistries and sequence motifs among circulating CM9-specific $CD8^+$ T cells from control and immunotoxin-treated macaques on day 20, representing the nadir of depletion (**Figure 3A**, **B**). Moreover, we found no significant differences in repertoire diversity measured using any of three distinct metrics, namely the number of unique clonotypes, the Shannon-Weiner index (34), or the d50 index (35), among circulating CM9-specific $CD8^+$ T cells from control versus immunotoxin-treated macaques after reconstitution (day 30) (**Figure 3C**–**E**). A similar overall picture was observed in BAL and LNs (**Figure 3C**–**E**). Using the TCR neighborhood enrichment test (TCRNET) (34), we identified enriched clonotypes in BAL (n = 9) and LNs (n = 3) from immunotoxin-treated versus control macaques on day 20 (**Figure 3F**), but no such differences were apparent on day 30 (**Figure 3G**). In similar comparisons of CM9-specific $CD8^+$ T cells isolated from PBMCs, no enriched clonotypes were detected on day 20 (**Figure 3F**), and very few clonotypes (n = 2) reached the threshold for significance on day 30 (**Figure 3G**). Multidimensional scaling (MDS) further revealed no obvious clustering by anatomical site, group, or time point (**Figure 3H**), and there was no obvious categorical segregation by TRBV or TRBJ segment use (**Supplemental Figure 2A**, **B**). These collective analyses indicated minimal perturbation and rapid normalization of the CM9-specific $CD8^+$ T cell repertoire after immunotoxin administration during acute infection with SIV.

Immunotoxin administration does not impact viral replication during or after treatment with ARVs

To evaluate the role of CM9-specific $CD8^+$ T cells during and after treatment with ARVs, we administered the immunotoxin to five chronically infected Mamu-A*01^+ rhesus macaques receiving a daily coformulated drug regimen comprising the nucleo(s/t)ide reverse transcriptase inhibitors emtricitabine (FTC) and tenofovir disoproxil fumarate (TDF), a prodrug of tenofovir (TFV), and the integrase strand-transfer inhibitor dolutegravir (DTG). Immunotoxin was withheld from five control Mamu-A*01^+ rhesus macaques treated otherwise identically. The dosing and sampling schedules are depicted in **Figure 4A**. Immunotoxin administration transiently reduced the frequencies of CM9-specific $CD8^+$ T cells among PBMCs (**Figure 4B**), but no corresponding effects were observed in BAL, colon, jejunum, or LNs (**Supplemental Figure 3A**–**D**). The frequencies of total memory $CD8^+$ T cells also remained largely unchanged among PBMCs (**Figure 4C**). In contrast, the frequencies of total memory $CD4^+$ T cells were higher in immunotoxin-treated versus control macaques across the observed time course (**Figure 4D**), but importantly, there were no corresponding differences in the frequencies of circulating $Ki67^+$ $CD4^+$ T cells before and after immunotoxin administration (**Figure 4E**). This latter observation suggested that depletion of CM9-specific $CD8^+$ T cells did not lead to reactive $CD4^+$ T cell proliferation in the presence of ARVs.

No significant differences in viremia were observed between control and immunotoxin-treated macaques during or after treatment with ARVs (**Figure 4F**). However, viral recrudescence was delayed in several macaques across both experimental groups after the cessation of ARVs, in some cases for as long as 6 to 12 months after study initiation, and generally occurred more rapidly after

immunotoxin administration (**Figure 4F**). Power calculations nonetheless indicated that a much larger cohort (*n* = 15 macaques per group) would have been required to detect a 5-fold increase in plasma VL. $CD4^+$ T cell-associated VLs were also largely unchanged before and after immunotoxin administration, indicating a lack of efficacy against tissue reservoirs of SIV (**Figure 4G**). These findings suggested that circulating CM9-specific $CD8^+$ T cells minimally affected viral replication during and after treatment with ARVs.

To determine if this lack of efficacy could be explained by mutational immune escape, we sequenced the CM9 epitope in plasma samples obtained 14 days after the cessation of ARVs. Wildtype sequences were detected almost exclusively (**Supplemental Figure 3E**). A similar pattern was observed in the immunotoxin-treated macaques with acute infection and the immunotoxin-treated macaques with chronic infection described above, with one exception (DFH4) (**Supplemental Figure 3E**). Accordingly, epitope variation could not account for the biological inefficacy of the immunotoxin during acute or chronic progressive infection, either in the absence or presence of ARVs.

In a previous study, $CD45RA^+$, $panKIR^+$, and/or $NKG2A^+$ virtual memory $CD8^+$ T (T_{VM}) cells were found to become more frequent in HIV-1-infected people during treatment with ARVs (36). T_{VM} cells also limited viral reactivation *ex vivo*, potentially explaining an associated diminution of the viral reservoir *in vivo* (36). In line with these findings, we detected elevated frequencies of $CD45RA^+$ $panKIR^+$ $NKG2A^-$ T_{VM} cells during versus after treatment with ARVs (**Supplemental Figure 4A**). Moreover, the frequencies of these cells were unaffected by immunotoxin administration (**Supplemental Figure 4B**, **C**), further confirming the specificity of this

intervention. These observations suggested that alternative modes of viral suppression, potentially including T_{VM} cell activity, were able to compensate for the lack of immune pressure exerted by CM9-specific $CD8^+$ T cells during and after treatment with ARVs.

Immunotoxin administration restructures the clonotypic repertoire of CM9-specific $CD8^+$ T cells during treatment with ARVs

In a final series of experiments, we used a high-throughput sequencing approach to characterize *TRB* gene rearrangements among CM9-specific $CD8^+$ T cell populations isolated from four chronically infected Mamu-A*01^+ rhesus macaques before and after immunotoxin administration in the continuous presence of ARVs. Scatterplot analysis spanning all anatomical sites revealed a shift in the repertoire and the appearance of new clonotypes after immunotoxin administration (**Figure 5A**). Tissue-specific analyses confirmed these findings and identified new clonotypes that became dominant in BAL and PBMCs (**Figure 5B**). Public clonotypes were common, especially before immunotoxin administration, but private clonotypes tended to reconstitute CM9-specific $CD8^+$ T cell populations after immunotoxin administration (**Figure 5C)**. Logo analysis revealed similar CDR3β amino acid chemistries and sequence motifs before and after immunotoxin administration (**Supplemental Figure 5A**, **B**). Repertoire diversity was also largely unchanged before and after immunotoxin administration (**Supplemental Figure 5C**–**E**), and there were no obvious concomitant perturbations in TRBV or TRBJ segment use (**Supplemental Figure 5F**, **G**). These observations suggested that immunotoxin administration enabled previously subdominant and often private clonotypes to reconstitute CM9-specific $CD8^+$ T cell populations in the continuous presence of ARVs.

DISCUSSION

In this study, we used a targeted immunotoxin to deplete CM9-specific $CD8^+$ T cells in Mamu-$A*01^+$ rhesus macaques during acute or chronic infection with SIVmac239, the latter either untreated or treated with ARVs. Our data revealed a key role for CM9-specific $CD8^+$ T cells as mediators of the rare natural controller phenotype but failed to demonstrate significant antiviral activity during acute or chronic progressive infection. We also found no evidence to support the notion that CM9-specific $CD8^+$ T cells help suppress viral replication during or after treatment with ARVs. More generally, our findings validated a promising approach to the depletion of antigen-specific $CD8^+$ T cells in a nonhuman primate model that could aid the discovery of immune determinants of protection against SIV and, by extension, HIV-1.

The early development of highly cytotoxic virus-specific $CD8^+$ T cells equipped with enhanced survival properties has been linked with spontaneous immune control of HIV-1 and SIV (37–39). In our model, even transient depletion of CM9-specific $CD8^+$ T cells in two macaques with naturally suppressed viremia led to a reactive increase in plasma VLs, suggesting a causal association between antiviral functionality and natural control of SIV. A more comprehensive evaluation was precluded by the fact that very few rhesus macaques (<1%) express Mamu-A*01 and control viral replication in the absence of ARVs (40). Our study was therefore limited from a statistical perspective, with power calculations indicating that hundreds of macaques would have been required to confirm a 10-fold increase in plasma VL. It should also be noted that we did not formally evaluate the functional properties of CM9-specific $CD8^+$ T cells before immunotoxin administration. The biological relevance of SIV-specific $CD8^+$ T cells *in vivo* has been addressed previously via wholesale depletion using antibodies directed against CD8α, which also eliminate NK cells, or CD8β (24, 41–43). These reagents efficiently deplete circulating $CD8^+$ T cells but

have lesser effects in tissues (21, 23, 44), akin to our findings with saporin-conjugated tetrameric complexes of CM9/Mamu-A*01. However, the elimination of $CD8^+$ T cells *en masse* results in the expansion of memory $CD4^+$ T cells to fill the induced homeostatic hole in the immune system, likely reflecting increased availability of interleukin (IL)-15 (45–47). This phenomenon could potentially enhance viral propagation, at least in the absence of ARVs (48). In contrast, our targeted approach did not elicit reactive $CD4^+$ T cell proliferation, eliminating this caveat to interpretation and enabling us to detect an effect confined to the natural controller phenotype, which appeared uniquely reliant on CM9-specific $CD8^+$ T cells to suppress the replication of SIV.

$CD8^+$ T cells target multiple epitopes during infection with SIV. In some cases, epitomized by the Tat epitope S/TL8, mutational escape occurs readily, but in other cases, epitomized by the Gag epitope CM9, mutational escape either requires compensatory amino acid substitutions and/or compromises viral replication (49, 50). Accordingly, it is perhaps not surprising that we were unable to identify a clear antiviral role for CM9-specific $CD8^+$ T cells during acute or chronic progressive infection, although it should be noted that immunotoxin-mediated depletion was not absolute using the protocol reported here, especially among tissue sites that sustain active replication of SIV. Likewise, we found no evidence to support a biologically relevant antiviral role for CM9-specific $CD8^+$ T cells during or after treatment with ARVs, barring a few minor increases in viral replication following immunotoxin administration, which mimicked the natural breakthrough pattern that occurs commonly in the continuous presence of ARVs (51). These results could be explained similarly by the availability of other target epitopes restricted by MHC class I. Antibody-mediated depletion studies have indeed shown that $CD8^+$ T cells can maintain viral suppression during treatment with ARVs (23) but are nonetheless unable to delay viral

recrudescence after treatment with ARVs (52). This latter observation aligns with our data and suggests that other immune cell types and/or tissue-localized SIV-specific $CD8^+$ T cells could limit viral replication in the immediate aftermath of treatment cessation, at least in the absence of functional exhaustion (36).

Immunotoxin administration transiently perturbed the clonotypic repertoire of CM9-specific $CD8^+$ T cells during acute infection and more profoundly altered the clonotypic repertoire of CM9-specific $CD8^+$ T cells during chronic infection in the continuous presence of ARVs. Repertoire fluctuations during the active depletion phase could be explained by differences in the susceptibility of individual clonotypes to cell death, tissue redistribution, and/or the preferential expansion of distinct clonotypes receiving optimal signals via the corresponding TCRs (1, 53). The emergence of new tissue-specific clonotypes in particular defined the repertoire perturbations induced by immunotoxin administration during treatment with ARVs. It is notable here that such immune flexibility under conditions of minimal but persistent antigenic drive, which could potentially be exploited therapeutically, appears to be a consistent feature of infection with SIV (33, 54).

The model presented here may prove useful in future studies designed to unravel the role of specificity as a determinant of $CD8^+$ T cell efficacy. Our approach could also be extended in principle to antigen-specific $CD4^+$ T cells and other infections beyond SIV. Ultimately, the ability to dissect the biological relevance of specific antigenic targets in nonhuman primates has the potential to inform the design of more effective recombinant vaccines against infectious agents of global concern, such as HIV-1 and SARS-CoV-2.

METHODS

Sex as a biological variable

Male and female rhesus macaques (*Macaca mulatta*) were eligible for inclusion. Biological outcomes were evaluated collectively. Study enrollment was based on the expression of Mamu-A*01.

Experimental design

For the acute infection study, five Mamu-A*01$^+$ rhesus macaques were infected intravenously with 3,000 $TCID_{50}$ of SIVmac239, indicated as day 0. An immunotoxin preparation comprising saporin-conjugated tetrameric complexes of CM9/Mamu-A*01 was then administered intravenously at a dose of 350 pmol/kg on days 7, 10, and 13. For the chronic infection study, five Mamu-A*01$^+$ rhesus macaques with established SIVmac239 infection were injected intravenously with the immunotoxin preparation either once at a dose of 500 pmol/kg, 1 nmol/kg, or 2 nmol/kg, or twice at a dose of 350 pmol/kg, separated by an interval of 4 days. For the ARV study, five Mamu-A*01$^+$ rhesus macaques received a coformulated subcutaneous drug regimen comprising the nucleo(s/t)ide reverse transcriptase inhibitors FTC and TDF, a prodrug of TFV, and the integrase strand-transfer inhibitor DTG once daily, starting approximately 3 months after infection with SIVmac239 (55). Once plasma VL was reduced to <50 copies/mL, which occurred approximately 3 months after the initiation of ARVs, the immunotoxin preparation was administered three times intravenously at a dose of 350 pmol/kg, separated by intervals of 3 days. BAL, biopsies of colon, jejunum, and LNs, and PBMCs were collected from each macaque before and after immunotoxin administration. An identical protocol was used to sample an equal number

of control macaques in the acute infection study and the ARV study. Details of all participant macaques are listed in **Supplemental Tables 1**–**3**.

CM9 monomer production and immunotoxin tetramerization

Biotinylated monomeric complexes of CM9/Mamu-A*01 were generated as described previously (32, 56). Cleanup was performed using Pierce High Capacity Endotoxin Removal Spin Columns (Thermo Fisher Scientific). Monomers were then passed through a polyethersulfone membrane filter (0.1 μm, Sartorius), and residual endotoxin levels were measured using a Pierce Chromogenic Endotoxin Quant Kit (Thermo Fisher Scientific). Saporin conjugation and tetramerization were achieved by adding streptavidin-ZAP (Advanced Targeting Systems) stepwise to the purified monomers at a final molar ratio of 1:4. The immunotoxin complex was then diluted in phosphate-buffered saline (HyClone) and passed through a sterile filter (0.2 μm, Thermo Fisher Scientific).

Flow cytometry and cell sorting

Single-cell suspensions were washed twice with phosphate-buffered saline (HyClone). SIV-specific $CD8^+$ T cells were identified using fluorochrome-conjugated pentameric complexes of CM9/Mamu-A*01 (ProImmune). Antibodies against cell surface markers used to identify and phenotype lymphocyte populations are detailed in **Supplemental Table 4**. Dead cells were excluded using a LIVE/DEAD Fixable Aqua Dead Cell Stain Kit (Thermo Fisher Scientific). Samples were acquired using an LSRFortessa (BD Biosciences) or a Cytek Aurora (Cytek Biosciences). Bulk $CD4^+$ T cells and SIV-specific $CD8^+$ T cells were sorted using a

FACSymphony S6 (BD Biosciences). The gating strategy is depicted in **Supplemental Figure 6**. All flow cytometry data were analyzed using FlowJo version 10.8.1 (FlowJo LLC).

Viral load quantification and CM9 epitope sequencing

Plasma VLs were quantified as described previously (55). $CD4^+$ T cell-associated VLs were determined relative to a housekeeping gene (albumin) using a FRugally Optimized DNA Octomer (FRODO) qPCR (57). Epitope sequencing from plasma samples was performed as described previously (58) using primers specific for the CM9 region (5'-CAGAAGTAGTGCCAGGATTTCAGG-3' and 5'-CTCTGATAATCTGCATAGCCGCTTG-3').

Clonotype analysis

Clonotype analysis was performed as described previously (33, 59). Briefly, SIV-specific $CD8^+$ T cells (n = 100–10,000) were sorted into 100 μL of RNAlater (Sigma-Aldrich), and *TRBV* gene rearrangements were amplified without bias using a template-switch anchored RT-PCR. Unique barcodes and the P5 and P7 sequencing adaptors (Illumina) were added to all amplification products using sequential PCRs. Sequences were generated using a paired-end (150 bp) strategy in conjunction with MiSeq v2 Kits (Illumina). TRBV and TRBJ segments were identified using MiXCR (60). Diversity and similarity indices were calculated using VDJtools (34). Graphs showing TRBV and TRBJ segment use, heatmaps, and scatter plots were also generated using VDJtools. MDS plots were graphed using RStudio version 1.3.1056. Clonotypes were defined by CDR3β amino acid sequence and TRBV/TRBJ (61, 62). Public clonotypes were defined as identical across more than one macaque in this study, also matching previously reported sequences

specific for CM9 (https://vdjdb.cdr3.net). Private clonotypes were identified in a single anatomical site in a single macaque. TCR repertoire plots were constructed to incorporate all sequences with a frequency of >2%.

Statistics

Experimental groups were compared using paired t-tests, area-under-the-curve (AUC) analyses, or various ANOVAs with post-hoc tests in Prism version 9.3.1 (GraphPad). Significance was assigned at $P < 0.05$.

Study approval

All experimental procedures were approved by the National Institute of Allergy and Infectious Diseases Animal Care and Use Committee as part of the Intramural Research Program of the National Institutes of Health (NIH protocol LVD 26E). In line with the Nonhuman Primate Management Plan set out by the Office of Animal Care and Use, macaques were housed at the NIH Animal Center under the supervision of the Division of Veterinary Resources, accredited by the Association for the Assessment and Accreditation of Laboratory Animal Care (AAALAC). Care at this facility met the advisory standards of the Animal Welfare Act and Animal Welfare Regulations, the United States Fish and Wildlife Services, and the Guide for the Care and Use of Laboratory Animals (8^{th} Edition). The physical condition of each macaque was monitored daily. Participant macaques were exempt from contact social housing on scientific grounds aligned with the respective protocol of the National Institute of Allergy and Infectious Diseases Animal Care and Use Committee. All macaques were therefore housed under noncontact social conditions for the duration of the study. Access to water was provided continuously. Commercial monkey

biscuits were offered twice daily, alongside fresh produce, bread and egg products, and a foraging mix consisting of raisins, nuts, and rice. Environmental enrichment to stimulate foraging and play activity was provided in the form of food puzzles, mirrors, toys, and cage furniture.

Data availability

TCR sequencing data have been deposited in the Sequence Read Archive (SRA) under accession number PRJNA906932 (https://www.ncbi.nlm.nih.gov/sra/PRJNA906932).

AUTHOR CONTRIBUTIONS

J.S. and J.M.B. designed the study. J.S., C.E.S., A.M.O., C.M.F., B.F.K., and J.M.B. performed experiments. J.S., S.D., C.M.F., and J.M.B. analyzed data. A.R., S.L.-L., D.C.D., and D.A.P. provided bespoke reagents and technical advice. J.S., D.A.P., and J.M.B. wrote the paper. All authors contributed intellectually and approved the final draft of the manuscript for publication.

ACKNOWLEDGEMENTS

We thank Kathryn Conway, Richard Herbert, Heather Kendall, and all veterinary staff at the NIH Animal Center. We also thank Jeff Lifson for assistance with the quantification of plasma VLs. The content of this publication does not necessarily reflect the views or policies of the Department of Health and Human Services, nor does the mention of trade names, commercial products, or organizations imply endorsement by the United States Government.

FUNDING STATEMENT

This study was funded by the Division of Intramural Research of the National Institute of Allergy and Infectious Diseases, NIH. D.A.P. was supported by a Wellcome Trust Senior Investigator Award (100326/Z/12/Z). J.M.B. was supported by the National Institute of Allergy and Infectious Diseases, NIH (1ZIAAI001029). Additional funds were provided by the National Cancer Institute, NIH (75N91019D00024). The funders had no role in study design, data collection, data analysis, preparation of the manuscript, or the decision to publish.

REFERENCES

1. Almeida JR, Price DA, Papagno L, Arkoub ZA, Sauce D, Bornstein E, et al. Superior control of HIV-1 replication by $CD8^+$ T cells is reflected by their avidity, polyfunctionality, and clonal turnover. *J Exp Med.* 2007;204(10):2473–85.
2. Hersperger AR, Migueles SA, Betts MR, and Connors M. Qualitative features of the HIV-specific $CD8^+$ T-cell response associated with immunologic control. *Curr Opin HIV AIDS.* 2011;6(3):169–73.
3. Klatt NR, Shudo E, Ortiz AM, Engram JC, Paiardini M, Lawson B, et al. $CD8^+$ lymphocytes control viral replication in SIVmac239-infected rhesus macaques without decreasing the lifespan of productively infected cells. *PLoS Pathog.* 2010;6(1):e1000747.
4. Rosati E, Dowds CM, Liaskou E, Henriksen EKK, Karlsen TH, and Franke A. Overview of methodologies for T-cell receptor repertoire analysis. *BMC Biotechnol.* 2017;17(1):61.
5. Wherry EJ, and Ahmed R. Memory CD8 T-cell differentiation during viral infection. *J Virol.* 2004;78(11):5535–45.
6. Hersperger AR, Pereyra F, Nason M, Demers K, Sheth P, Shin LY, et al. Perforin expression directly ex vivo by HIV-specific $CD8^+$ T-cells is a correlate of HIV elite control. *PLoS Pathog.* 2010;6(5):e1000917.
7. Nowacki TM, Kuerten S, Zhang W, Shive CL, Kreher CR, Boehm BO, et al. Granzyme B production distinguishes recently activated $CD8^+$ memory cells from resting memory cells. *Cell Immunol.* 2007;247(1):36–48.
8. Appay V, Nixon DF, Donahoe SM, Gillespie GMA, Dong T, King A, et al. HIV-specific $CD8^+$ T cells produce antiviral cytokines but are impaired in cytolytic function. *J Exp Med.* 2000;192(1):63–76.
9. Bachmann MF, Barner M, Viola A, and Kopf M. Distinct kinetics of cytokine production and cytolysis in effector and memory T cells after viral infection. *Eur J Immunol.* 1999;29(1):291–9.
10. Koup RA, Safrit JT, Cao Y, Andrews CA, McLeod G, Borkowsky W, et al. Temporal association of cellular immune responses with the initial control of viremia in primary human immunodeficiency virus type 1 syndrome. *J Virol.* 1994;68(7):4650–5.
11. Chen ZW, Craiu A, Shen L, Kuroda MJ, Iroku UC, Watkins DI, et al. Simian immunodeficiency virus evades a dominant epitope-specific cytotoxic T lymphocyte response through a mutation resulting in the accelerated dissociation of viral peptide and MHC class I. *J Immunol.* 2000;164(12):6474–9.
12. Oxenius A, Price DA, Trkola A, Edwards C, Gostick E, Zhang HT, et al. Loss of viral control in early HIV-1 infection is temporally associated with sequential escape from $CD8^+$ T cell responses and decrease in HIV-1-specific $CD4^+$ and $CD8^+$ T cell frequencies. *J Infect Dis.* 2004;190(4):713–21.
13. Price DA, West SM, Betts MR, Ruff LE, Brenchley JM, Ambrozak DR, et al. T cell receptor recognition motifs govern immune escape patterns in acute SIV infection. *Immunity.* 2004;21(6):793–803.
14. Borrow P, Lewicki H, Wei X, Horwitz MS, Peffer N, Meyers H, et al. Antiviral pressure exerted by HIV-1-specific cytotoxic T lymphocytes (CTLs) during primary infection demonstrated by rapid selection of CTL escape virus. *Nat Med.* 1997;3(2):205–11.

15. Price DA, Goulder PJ, Klenerman P, Sewell AK, Easterbrook PJ, Troop M, et al. Positive selection of HIV-1 cytotoxic T lymphocyte escape variants during primary infection. *Proc Natl Acad Sci U S A.* 1997;94(5):1890–5.
16. Allen TM, O'Connor DH, Jing P, Dzuris JL, Mothé BR, Vogel TU, et al. Tat-specific cytotoxic T lymphocytes select for SIV escape variants during resolution of primary viraemia. *Nature.* 2000;407(6802):386–90.
17. Walter L, and Ansari AA. MHC and KIR polymorphisms in rhesus macaque SIV infection. *Front Immunol.* 2015;6:540.
18. Carrington M, Bashirova AA, and McLaren PJ. On stand by: host genetics of HIV control. *AIDS.* 2013;27(18):2831–9.
19. Stephens HA. HIV-1 diversity versus HLA class I polymorphism. *Trends Immunol.* 2005;26(1):41–7.
20. Mudd PA, Martins MA, Ericsen AJ, Tully DC, Power KA, Bean AT, et al. Vaccine-induced $CD8^+$ T cells control AIDS virus replication. *Nature.* 2012;491(7422):129–33.
21. McBrien JB, Kumar NA, and Silvestri G. Mechanisms of $CD8^+$ T cell-mediated suppression of HIV/SIV replication. *Eur J Immunol.* 2018;48(6):898–914.
22. Chowdhury A, Hayes TL, Bosinger SE, Lawson BO, Vanderford T, Schmitz JE, et al. Differential impact of in vivo $CD8^+$ T lymphocyte depletion in controller versus progressor simian immunodeficiency virus-infected macaques. *J Virol.* 2015;89(17):8677–86.
23. Cartwright EK, Spicer L, Smith SA, Lee D, Fast R, Paganini S, et al. $CD8^+$ lymphocytes are required for maintaining viral suppression in SIV-infected macaques treated with short-term antiretroviral therapy. *Immunity.* 2016;45(3):656–68.
24. Matano T, Shibata R, Siemon C, Connors M, Lane HC, and Martin MA. Administration of an anti-CD8 monoclonal antibody interferes with the clearance of chimeric simian/human immunodeficiency virus during primary infections of rhesus macaques. *J Virol.* 1998;72(1):164–9.
25. Mueller YM, Do DH, Boyer JD, Kader M, Mattapallil JJ, Lewis MG, et al. $CD8^+$ cell depletion of SHIV89.6P-infected macaques induces $CD4^+$ T cell proliferation that contributes to increased viral loads. *J Immunol.* 2009;183(8):5006–12.
26. Polito L, Bortolotti M, Farini V, Battelli MG, Barbieri L, and Bolognesi A. Saporin induces multiple death pathways in lymphoma cells with different intensity and timing as compared to ricin. *Int J Biochem Cell Biol.* 2009;41(5):1055–61.
27. Hess PR, Barnes C, Woolard MD, Johnson MDL, Cullen JM, Collins EJ, et al. Selective deletion of antigen-specific $CD8^+$ T cells by MHC class I tetramers coupled to the type I ribosome-inactivating protein saporin. *Blood.* 2007;109(8):3300–7.
28. Leitman EM, Palmer CD, Buus S, Chen F, Riddell L, Sims S, et al. Saporin-conjugated tetramers identify efficacious anti-HIV $CD8^+$ T-cell specificities. *PLoS One.* 2017;12(10):e0184496.
29. Casimiro DR, Wang F, Schleif WA, Liang X, Zhang ZQ, Tobery TW, et al. Attenuation of simian immunodeficiency virus SIVmac239 infection by prophylactic immunization with DNA and recombinant adenoviral vaccine vectors expressing Gag. *J Virol.* 2005;79(24):15547–55.

30. Peyerl FW, Barouch DH, Yeh WW, Bazick HS, Kunstman J, Kunstman KJ, et al. Simian-human immunodeficiency virus escape from cytotoxic T-lymphocyte recognition at a structurally constrained epitope. *J Virol.* 2003;77(23):12572–8.
31. Peyerl FW, Bazick HS, Newberg MH, Barouch DH, Sodroski J, and Letvin NL. Fitness costs limit viral escape from cytotoxic T lymphocytes at a structurally constrained epitope. *J Virol.* 2004;78(24):13901–10.
32. Price DA, Asher TE, Wilson NA, Nason MC, Brenchley JM, Metzler IS, et al. Public clonotype usage identifies protective Gag-specific $CD8^+$ T cell responses in SIV infection. *J Exp Med.* 2009;206(4):923–36.
33. Simpson J, Starke CE, Ortiz AM, Ransier A, Darko S, Douek DC, et al. Multiple modes of antigen exposure induce clonotypically diverse epitope-specific $CD8^+$ T cells across multiple tissues in nonhuman primates. *PLoS Pathog.* 2022;18(7):e1010611.
34. Shugay M, Bagaev DV, Turchaninova MA, Bolotin DA, Britanova OV, Putintseva EV, et al. VDJtools: unifying post-analysis of T cell receptor repertoires. *PLoS Comput Biol.* 2015;11(11):e1004503.
35. Hou XL, Wang L, Ding YL, Xie Q, and Diao HY. Current status and recent advances of next generation sequencing techniques in immunological repertoire. *Genes Immun.* 2016;17(3):153–64.
36. Jin JH, Huang HH, Zhou MJ, Li J, Hu W, Huang L, et al. Virtual memory $CD8^+$ T cells restrain the viral reservoir in HIV-1-infected patients with antiretroviral therapy through derepressing KIR-mediated inhibition. *Cell Mol Immunol.* 2020;17(12):1257–65.
37. Passaes C, Millet A, Madelain V, Monceaux V, David A, Versmisse P, et al. Optimal maturation of the SIV-specific $CD8^+$ T cell response after primary infection is associated with natural control of SIV: ANRS SIC Study. *Cell Rep.* 2020;32(12):108174.
38. Yan J, Sabbaj S, Bansal A, Amatya N, Shacka JJ, Goepfert PA, et al. HIV-specific $CD8^+$ T cells from elite controllers are primed for survival. *J Virol.* 2013;87(9):5170–81.
39. Hersperger AR, Martin JN, Shin LY, Sheth PM, Kovacs CM, Cosma GL, et al. Increased HIV-specific $CD8^+$ T-cell cytotoxic potential in HIV elite controllers is associated with T-bet expression. *Blood.* 2011;117(14):3799–808.
40. Mothe BR, Weinfurter J, Wang C, Rehrauer W, Wilson N, Allen TM, et al. Expression of the major histocompatibility complex class I molecule Mamu-A*01 is associated with control of simian immunodeficiency virus SIVmac239 replication. *J Virol.* 2003;77(4):2736–40.
41. Wong JK, Strain MC, Porrata R, Reay E, Sankaran-Walters S, Ignacio CC, et al. In vivo $CD8^+$ T-cell suppression of SIV viremia is not mediated by CTL clearance of productively infected cells. *PLoS Pathog.* 2010;6(1):e1000748.
42. McBrien JB, Wong AKH, White E, Carnathan DG, Lee JH, Safrit JT, et al. Combination of CD8β depletion and interleukin-15 superagonist N-803 induces virus reactivation in simian-human immunodeficiency virus-infected, long-term ART-treated rhesus macaques. *J Virol.* 2020;94(19):e00755-20.
43. Choi EI, Reimann KA, and Letvin NL. In vivo natural killer cell depletion during primary simian immunodeficiency virus infection in rhesus monkeys. *J Virol.* 2008;82(13):6758–61.

44. McBrien JB, Mavigner M, Franchitti L, Smith SA, White E, Tharp GK, et al. Robust and persistent reactivation of SIV and HIV by N-803 and depletion of $CD8^+$ cells. *Nature.* 2020;578(7793):154–9.
45. Okoye AA, DeGottardi MQ, Fukazawa Y, Vaidya M, Abana CO, Konfe AL, et al. Role of IL-15 signaling in the pathogenesis of simian immunodeficiency virus infection in rhesus macaques. *J Immunol.* 2019;203(11):2928–43.
46. DeGottardi MQ, Okoye AA, Vaidya M, Talla A, Konfe AL, Reyes MD, et al. Effect of anti-IL-15 administration on T cell and NK cell homeostasis in rhesus macaques. *J Immunol.* 2016;197(4):1183–98.
47. Okoye A, Park H, Rohankhedkar M, Coyne-Johnson L, Lum R, Walker JM, et al. Profound $CD4^+$/$CCR5^+$ T cell expansion is induced by $CD8^+$ lymphocyte depletion but does not account for accelerated SIV pathogenesis. *J Exp Med.* 2009;206(7):1575–88.
48. Statzu M, Jin W, Fray EJ, Wong AKH, Kumar MR, Ferrer E, et al. $CD8^+$ lymphocytes do not impact SIV reservoir establishment under ART. *Nat Microbiol.* 2023;8(2):299–308.
49. Vanderford TH, Bleckwehl C, Engram JC, Dunham RM, Klatt NR, Feinberg MB, et al. Viral CTL escape mutants are generated in lymph nodes and subsequently become fixed in plasma and rectal mucosa during acute SIV infection of macaques. *PLoS Pathog.* 2011;7(5):e1002048.
50. Friedrich TC, Frye CA, Yant LJ, O'Connor DH, Kriewaldt NA, Benson M, et al. Extraepitopic compensatory substitutions partially restore fitness to simian immunodeficiency virus variants that escape from an immunodominant cytotoxic-T-lymphocyte response. *J Virol.* 2004;78(5):2581–5.
51. Del Prete GQ, Alvord WG, Li Y, Deleage C, Nag M, Oswald K, et al. TLR7 agonist administration to SIV-infected macaques receiving early initiated cART does not induce plasma viremia. *JCI Insight.* 2019;4(11):e127717.
52. Okoye AA, Duell DD, Fukazawa Y, Varco-Merth B, Marenco A, Behrens H, et al. $CD8^+$ T cells fail to limit SIV reactivation following ART withdrawal until after viral amplification. *J Clin Invest.* 2021;131(8):e141677.
53. Lee K-H, Dinner AR, Tu C, Campi G, Raychaudhuri S, Varma R, et al. The immunological synapse balances T cell receptor signaling and degradation. *Science.* 2003;302(5648):1218–22.
54. Heather JM, Best K, Oakes T, Gray ER, Roe JK, Thomas N, et al. Dynamic perturbations of the T-cell receptor repertoire in chronic HIV infection and following antiretroviral therapy. *Front Immunol.* 2016;6:644.
55. Ortiz AM, Flynn JK, DiNapoli SR, Vujkovic-Cvijin I, Starke CE, Lai SH, et al. Experimental microbial dysbiosis does not promote disease progression in SIV-infected macaques. *Nat Med.* 2018;24(9):1313–6.
56. Kuroda MJ, Schmitz JE, Barouch DH, Craiu A, Allen TM, Sette A, et al. Analysis of Gag-specific cytotoxic T lymphocytes in simian immunodeficiency virus–infected rhesus monkeys by cell staining with a tetrameric major histocompatibility complex class I–peptide complex. *J Exp Med.* 1998;187(9):1373–81.
57. Langner CA, and Brenchley JM. FRugally Optimized DNA Octomer (FRODO) qPCR measurement of HIV and SIV in human and nonhuman primate samples. *Curr Protoc.* 2021;1(4):e93.

58. Immonen TT, Camus C, Reid C, Fennessey CM, Del Prete GQ, Davenport MP, et al. Genetically barcoded SIV reveals the emergence of escape mutations in multiple viral lineages during immune escape. *Proc Natl Acad Sci U S A.* 2020;117(1):494–502.
59. Quigley MF, Almeida JR, Price DA, and Douek DC. Unbiased molecular analysis of T cell receptor expression using template-switch anchored RT-PCR. *Curr Protoc Immunol.* 2011;Chapter 10:Unit10.33.
60. Bolotin DA, Poslavsky S, Mitrophanov I, Shugay M, Mamedov IZ, Putintseva EV, et al. MiXCR: software for comprehensive adaptive immunity profiling. *Nat Methods.* 2015;12(5):380–1.
61. Yassai MB, Naumov YN, Naumova EN, and Gorski J. A clonotype nomenclature for T cell receptors. *Immunogenetics.* 2009;61(7):493–502.
62. Greenaway HY, Kurniawan M, Price DA, Douek DC, Davenport MP, and Venturi V. Extraction and characterization of the rhesus macaque T-cell receptor β-chain genes. *Immunol Cell Biol.* 2009;87(7):546–53.

FIGURE LEGENDS

Figure 1

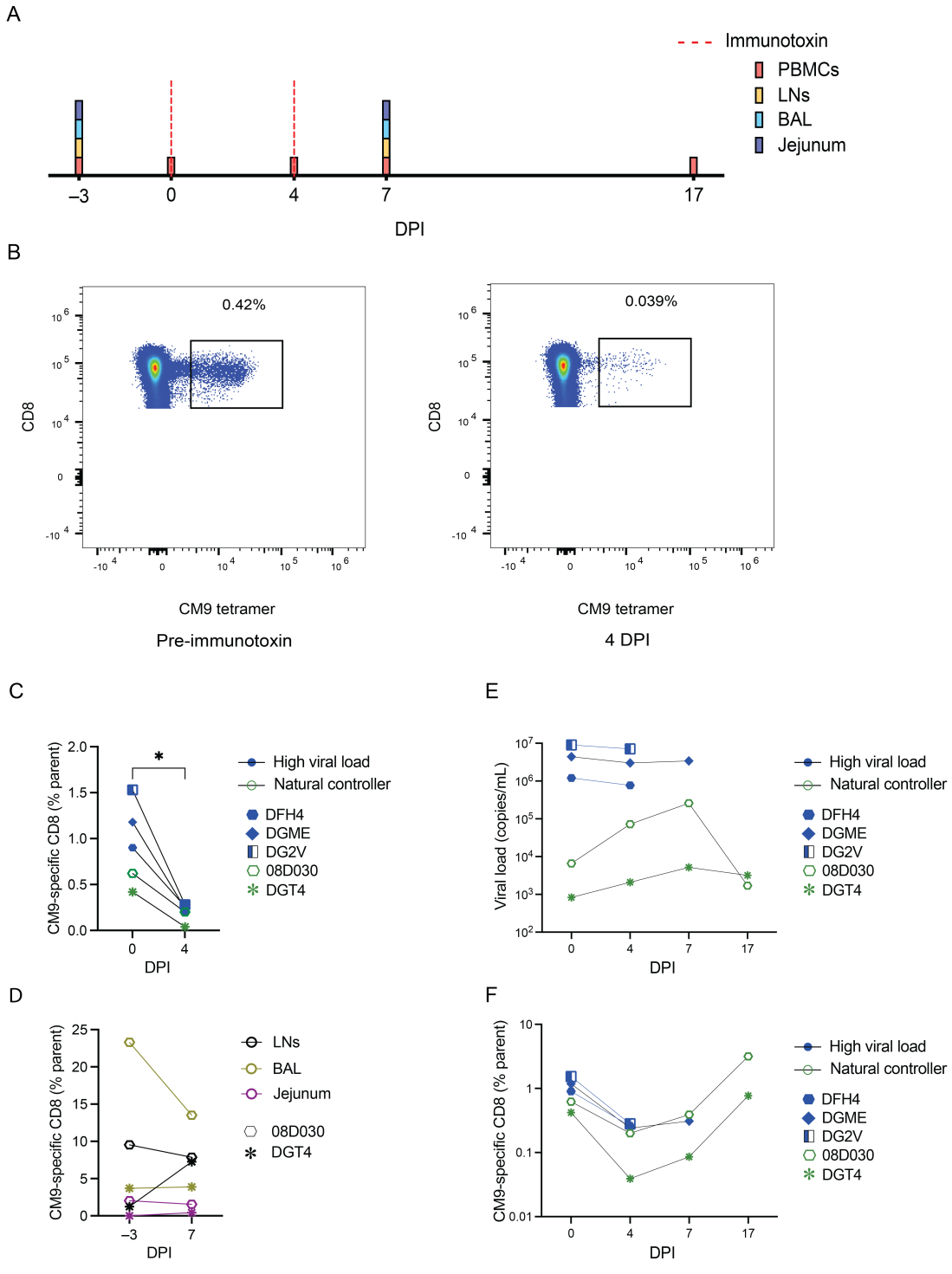

Figure 1. CM9-specific CD8$^+$ T cells contribute to natural control of viremia during chronic infection with SIV. (**A**) Schematic representation of the experiment. Immunotoxin was administered to five Mamu-A*01$^+$ rhesus macaques chronically infected with SIVmac239. (**B**) Representative flow cytometry plots showing CM9 tetramer staining versus CD8. Plots are gated on live memory CD8$^+$ events. (**C**) CM9-specific CD8$^+$ T cell frequencies among PBMCs (parent = CD8$^+$ T cells). (**D**) CM9-specific CD8$^+$ T cell frequencies in BAL, jejunum, and LNs (parent = CD8$^+$ T cells). (**E**) Plasma VLs. (**F**) Extended quantification of CM9-specific CD8$^+$ T cell frequencies among PBMCs (parent = CD8$^+$ T cells). Each symbol represents one macaque (C–F). Significance was determined using a paired t-test (C, D). *$P < 0.05$. DPI, days post-immunotoxin.

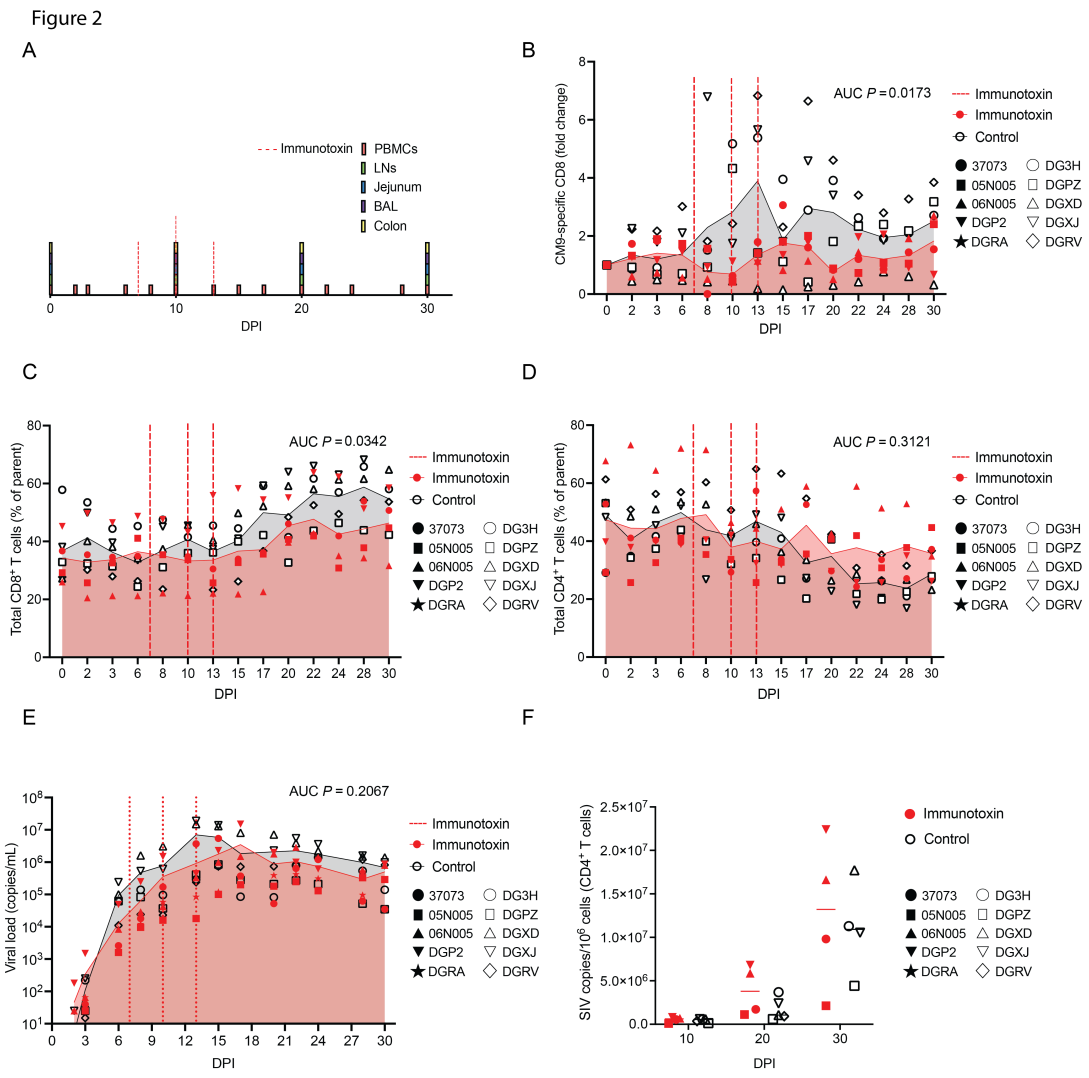

Figure 2. Immunotoxin administration does not alter viral load kinetics during acute infection with SIV. (**A**) Schematic representation of the experiment. Immunotoxin was administered to five Mamu-A*01^{+} rhesus macaques acutely infected with SIVmac239. Immunotoxin was withheld from five control Mamu-A*01^{+} rhesus macaques treated otherwise identically. (**B**) CM9-specific CD8^{+} T cell frequencies among PBMCs (fold change). (**C**) Total memory CD8^{+} T cell frequencies among PBMCs (parent = memory T cells). (**D**) Total memory CD4^{+} T cell frequencies among PBMCs (parent = memory T cells). (**E**) Plasma VLs. (**F**) CD4^{+} T

cell-associated VLs. Each symbol represents one macaque (B–F). Shaded areas depict mean values (B–E). Horizontal bars indicate median values (F). Significance was determined using AUC analysis (B–E) or a mixed-effects ANOVA with Šídák correction (F). DPI, days post-infection.

Figure 3

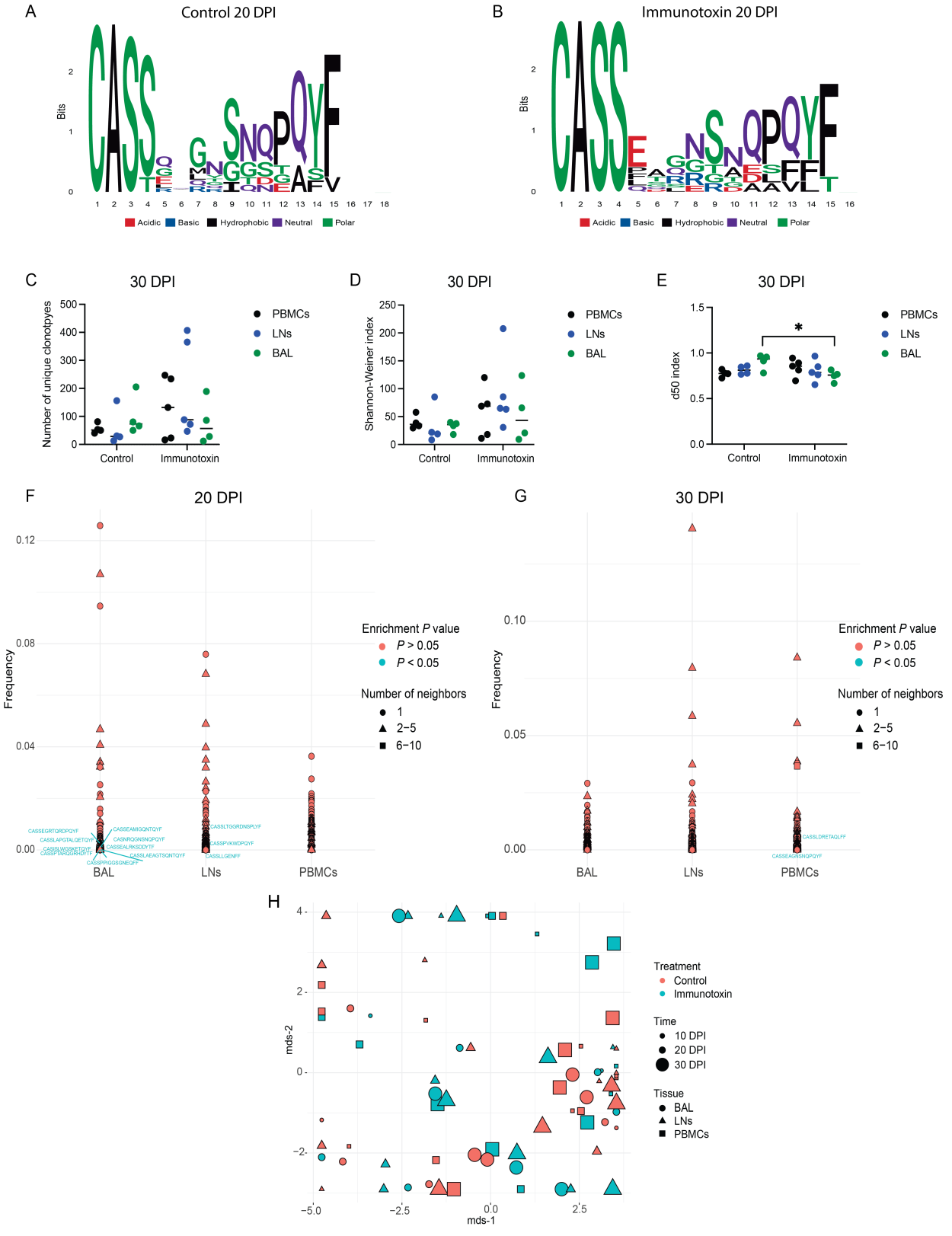
A
Control 20 DPI
Bits
Acidic
Basic
Hydrophobic
Neutral
Polar
B
Immunotoxin 20 DPI
C
30 DPI
Number of unique clonotypes
PBMCs
LNs
BAL
Control
Immunotoxin
D
30 DPI
Shannon-Weiner index
E
30 DPI
d50 index
F
20 DPI
Frequency
Enrichment P value
P > 0.05
P < 0.05
Number of neighbors
1
2–5
6–10
BAL
LNs
PBMCs
G
30 DPI
H
mds-1
mds-2
Treatment
Control
Immunotoxin
Time
10 DPI
20 DPI
30 DPI
Tissue

Figure 3. Immunotoxin administration does not modulate the clonotypic repertoire of CM9-specific CD8$^+$ T cells during acute infection with SIV. Experimental details as in **Figure 2**. (**A**) Logo plots and chemical classification of amino acids spanning the CDR3β loops of the top 10 pooled clonotypes from control macaques on day 20. (**B**) Logo plots and chemical classification of amino acids spanning the CDR3β loops of the top 10 pooled clonotypes from immunotoxin-treated macaques on day 20. (**C**) Repertoire diversity measured using the number of unique clonotypes for CM9-specific CD8$^+$ T cell populations from control and immunotoxin-treated macaques on day 30. (**D**) Repertoire diversity measured using the Shannon-Weiner index for CM9-specific CD8$^+$ T cell populations from control and immunotoxin-treated macaques on day 30. (**E**) Repertoire diversity measured using the d50 index for CM9-specific CD8$^+$ T cell populations from control and immunotoxin-treated macaques on day 30. (**F**) TCRNET analysis of CM9-specific CD8$^+$ T cell repertoires from control and immunotoxin-treated macaques on day 20. (**G**) TCRNET analysis of CM9-specific CD8$^+$ T cell repertoires from control and immunotoxin-treated macaques on day 30. (**H**) MDS analysis of CM9-specific CD8$^+$ T cell repertoires from control and immunotoxin-treated macaques on days 10, 20, and 30. Clonotypes that were enriched in CM9-specific CD8$^+$ T cell populations from immunotoxin-treated macaques are shown in blue. Each symbol represents one macaque (C–E, H). Horizontal bars indicate median values (C–E). Significance was determined using a two-way ANOVA with Šídák correction (C–E). *$P < 0.05$. DPI, days post-infection.

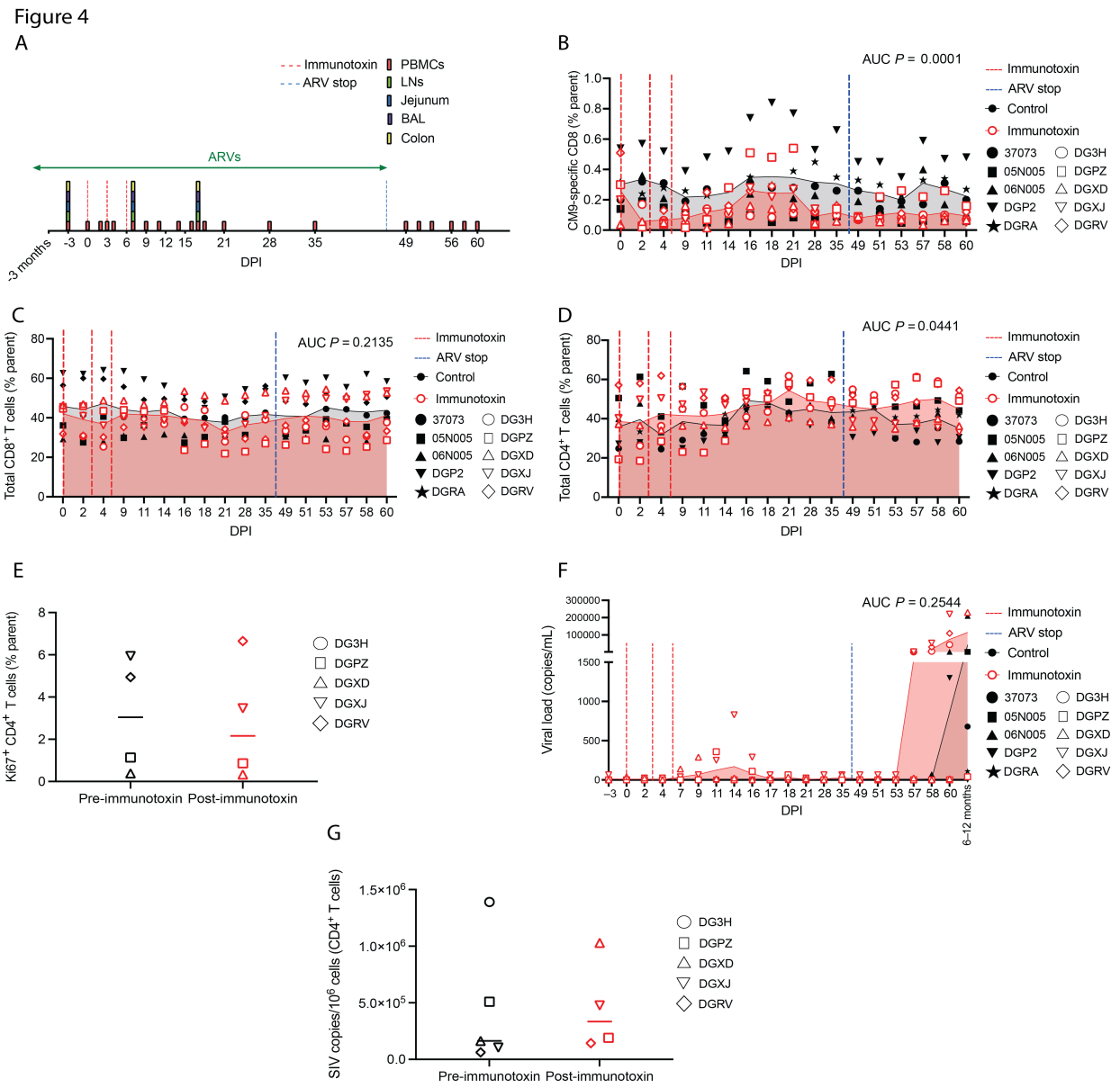

Figure 4. Immunotoxin administration does not impact viral replication during or after treatment with ARVs. (**A**) Schematic representation of the experiment. Immunotoxin was administered to five Mamu-A*01^{+} rhesus macaques chronically infected with SIVmac239 undergoing continuous treatment with ARVs. Immunotoxin was withheld from five control Mamu-A*01^{+} rhesus macaques treated otherwise identically. (**B**) CM9-specific CD8^{+} T cell frequencies among PBMCs (parent = CD8^{+} T cells). (**C**) Total memory CD8^{+} T cell frequencies

among PBMCs (parent = memory T cells). (**D**) Total memory $CD4^+$ T cell frequencies among PBMCs (parent = memory T cells). (**E**) $Ki67^+$ $CD4^+$ T cell frequencies among PBMCs (parent = $CD4^+$ T cells). (**F**) Plasma VLs. (**G**) $CD4^+$ T cell-associated VLs. Each symbol represents one macaque (B–G). Shaded areas depict mean values (B–D, F). Horizontal bars indicate median values (E, G). Significance was determined using AUC analysis (B–D, F) or a paired t-test (E, G). Post-immunotoxin = day 7 (E, G). DPI, days post-immunotoxin.

Figure 5

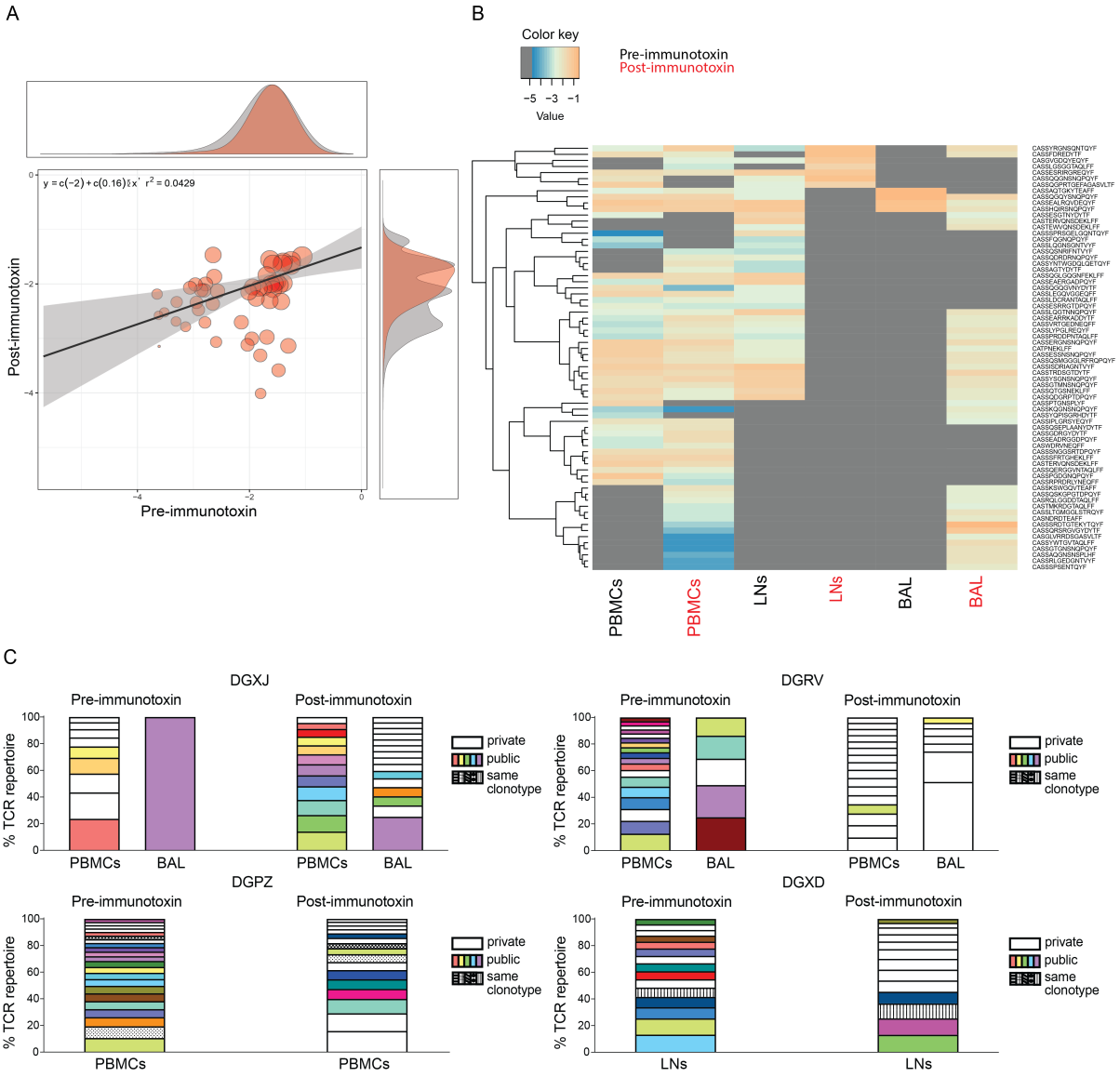

Figure 5. Immunotoxin administration restructures the clonotypic repertoire of CM9-specific CD8$^+$ T cells during treatment with ARVs. Experimental details as in **Figure 4**. (**A**) Scatterplot analysis of CM9-specific CD8$^+$ T cell repertoires spanning all macaques and all anatomical sites before and after immunotoxin administration. (**B**) Heatmap analysis of CM9-specific CD8$^+$ T cell repertoires spanning all macaques and each anatomical site before and after immunotoxin administration. (**C**) Public and private clonotype frequencies among CM9-specific

$CD8^+$ T cell populations from individual macaques (n = 4). Plots incorporate all sequences with a frequency of >2%. Post-immunotoxin = day 7 (A–C).